

The infinite-range quantum random Heisenberg magnet.

Liliana Arrachea^{1,2} and Marcelo J. Rozenberg¹

¹ *Departamento de Física,*

FCEyN Universidad de Buenos Aires

Pabellón I, Ciudad Universitaria, (1428) Buenos Aires, Argentina.

² *Scuola Internazionale Superiore di Studi Avanzati (SISSA) and Istituto Nazionale per la Fisica della Materia (INFN)
Unità di Ricerca Trieste-SISSA, Via Beirut 4, I-34014 Trieste, Italy.*

(Received October 24, 2018)

We study with exact diagonalization techniques the Heisenberg model for a system of $SU(2)$ spins with $S = 1/2$ and random infinite-range exchange interactions. We calculate the critical temperature T_g for the spin-glass to paramagnetic transition. We obtain $T_g \approx 0.13$, in good agreement with previous quantum Monte Carlo and analytical estimates. We provide a detailed picture for the different kind of excitations which intervene in the dynamical response $\chi''(\omega, T)$ at $T = 0$ and analyze their evolution as T increases. We also calculate the specific heat $C_v(T)$. We find that it displays a smooth maximum at $T_M \approx 0.25$, in good qualitative agreement with experiments. We argue that the fact that $T_M > T_g$ is due to a quantum disorder effect.

I. INTRODUCTION

The physics of disordered magnets is a fascinating subject of condensed matter physics. Traditionally, two main ingredients are singled out as crucial to set the physical behavior of these systems: strong interaction and frustration. It is well known that the interplay between them leads to a rich variety of magnetically ordered phases, including conventional commensurate or incommensurate spin-density waves as well as the more exotic spin-glass state. The latter is characterized by an ordered magnetic state with permanent magnetic moments in the microscopic scale, but randomly oriented producing a vanishing net macroscopic magnetization. While the concept of spin itself is purely quantum, it is often maintained that quantum fluctuations are not important for spin-glass physics [1]. However, recent experiments have put the role of quantum fluctuations [2] at the center of the stage.

One example of real systems with a spin-glass phase at low temperature is the compound $\text{Li}_{1-x}\text{Ho}_x\text{YF}_4$ which is a dipolar coupled random magnet [3] and has been recently the focus of beautiful experiments [4] that introduced quantum fluctuations by means of an external transverse magnetic field. Another notable example is the LiV_2O_4 [5] compound in which the magnetic V atoms are placed at the vertices of a pyrochlore-like structure which produces strong frustration and a spin-glass state. The V d -electrons also form a very narrow conduction band that behaves as a strongly renormalized Fermi liquid, with parameters comparable to those of the so called heavy fermion compounds that usually involve only f -electrons. The likely connection between this observation and the spin-glass state remains a challenging open question. Finally, we have the cuprate superconductors, with vast experimental evidence that a glassy phase exists at low temperatures within a narrow range of doping concentrations between the antiferromagnetic and superconducting phases [6].

Much effort has been dedicated to investigate the spin-glass physics, and many ingenious and insightful theoretical ideas have contributed to our current understanding [1,2,7–9]. Nevertheless, despite this effort, many fundamental questions remain unsolved and the role of quantum fluctuations is only beginning to receive due attention. Among the many long-standing unresolved issues of spin-glass physics we can mention the intriguing behavior of the specific heat. In fact, experiments show that this quantity systematically has a maximum well above the spin-glass freezing temperature T_g [1,8]. It is usually claimed that quantum mechanical effects are not essential for the physical phenomena related with the spin-glass phase [1]. However, we shall later argue that precisely quantum effects might be at the origin of this long-standing puzzle.

Theoretical progress in the description of the glassy phase is usually prevented by technical difficulties. In particular, most of the analytical and numerical approaches rely on the so called replica trick [9]. Unfortunately, this clever technique becomes usually impractical within the glassy phase when replica symmetry breaking occurs. In a recent paper [10] we introduced the use of the method of numerical exact diagonalization of finite size clusters to investigate models of quantum random magnets at $T = 0$. This approach has two main advantages: (i) Averages over disorder can be directly performed, avoiding the use of replicas. In fact, the same effort is required to tackle both the disordered and the spin-glass ordered phases. (ii) The dynamical response is directly calculated on the real frequency axis and, unlike other numerical techniques such as quantum Monte Carlo, no analytical continuation from the imaginary axis is necessary. Another advantage is that unlike usual exact diagonalization calculations that give just a few poles in the response functions, in our case we obtain smooth functions due to the average over the disorder. However, the main drawback of this numerical method is that systems with a rather small number of spins are tractable. Nevertheless, this technical obstacle can be overcome by a careful finite size analysis. In fact, we found that most of the relevant physical quantities exhibit a smooth behavior as a function of the system size, and reliable extrapolations to the thermodynamic limit can be obtained [10,11]. Moreover, as we have complete knowledge of the system for every realization, including the ground state wave function, we can look at its structure to try to gain new insights. This has indeed turned out to be a useful idea, as we obtain an appealing physical picture of the low energy excitations of the spin-glass state, that would have not emerged from classical model numerical calculations.

In this work we consider the $\text{SU}(2)$ Heisenberg model for a system of $S = 1/2$ spins with random infinite-range exchange random interactions. It is defined by the hamiltonian

$$H = \frac{1}{\sqrt{N}} \sum_{i,j=1}^N J_{ij} \mathbf{S}_i \cdot \mathbf{S}_j, \quad (1)$$

where i, j labels sites of a lattice with N spins, \mathbf{S} denote the $\text{SU}(2)$ spin $1/2$ operators and the infinite-range exchange constants J_{ij} are normally distributed with variance J^2 that we set to unity. The phase diagram of this model was first outlined by Bray and Moore [12], who argued that a glassy phase should exist at low temperature for all values of S . These authors proposed an approach which is formulated on the imaginary time axis and uses the replica trick to obtain a set of self-consistent dynamical mean-field equations. The exact numerical solution of these equations was later obtained with quantum Monte Carlo techniques in the paramagnetic phase [13], and the solution was found

to become unstable towards spin-glass order at a critical temperature $T_g \approx 0.14J$. The study of $SU(M)$ extensions of this model has been treated in the limit of $M \rightarrow \infty$ [14–16], and spin-glass and spin-liquid phases were found at sufficiently low temperatures.

We have recently investigated the dynamical response of the hamiltonian (1) at zero temperature with exact diagonalization techniques [10]. We were able to describe in detail the structure of the ground state and the nature of the elemental excitations within the glassy phase. We found compelling evidence that the dynamical spin response behaves as $\chi''_{loc}(\omega) \sim q\delta(\omega) + \chi_{reg}(\omega)$ in the thermodynamic limit. We estimated $q \sim 0.06$ for the value of the Edwards-Anderson order parameter.

The aim of this paper is to extend the methodology based in exact diagonalization to investigate the physical behavior of the disordered Heisenberg model (1) at finite temperature. Our main goal is to achieve a detailed understanding of the different kind of excitations which occur in the dynamical spin response at different temperatures, within and above the glassy phase. We shall show that the regular part $\chi_{reg}(\omega)$ is in fact dominated by spin excitations due to quantum disorder. This contribution to the response function can be qualitatively understood in the framework of an heuristic mean-field theory that we present. Moreover, its functional form is very similar to that of the quantum spin-liquid discussed in Refs. [14–16] for the $SU(M)$ generalization of the Heisenberg model in the regime of large M and small S . We also investigate the behavior of the specific heat C_v as a function of temperature. We find that this quantity displays a smooth maximum at a temperature T_M well above the freezing temperature T_g , and we link this fact to the presence of strong quantum fluctuations. Interestingly, the unconventional behavior of the specific heat is in accordance with the observation of this effect in real materials that have a spin-glass state at low temperatures and remained unexplained so far.

The paper is organized as follows. In Section II we explain the numerical method and some technical details. Section III contains the study of the dynamical spin response. Results for the specific heat C_v are shown and discussed in Section IV. The summary and conclusions are presented in the Section V.

II. METHODOLOGY.

The general strategy is to take samples from the random ensemble of systems of size N and exactly diagonalize the ensuing hamiltonians (1). The different physical quantities are computed for each realization and then averaged over the number of samples. Finite size effects are analyzed and results are extrapolated to the thermodynamic limit. Typically, systems with up to $N = 17$ spins are solved at $T = 0$ and up to $N = 12$ at finite T . Averages are performed over several thousands to hundreds of thousands of disorder realizations. A typical run demands up to a week for the larger systems on an 8 node parallel cluster.

The ground state and the dynamical correlation functions at $T = 0$ are calculated by the Lanczos method [17]. It is convenient to take advantage of the $SU(2)$ symmetry of the model. The selected basis of states belongs to the $S^z = 0$ representation, where S^z is the quantum number corresponding to the z -component of the total spin. A projector is used to find the ground state within each subspace with total spin S [18]. The local spin susceptibility is obtained from

$$\chi_{loc}(\omega) = \frac{1}{M} \sum_{m=1}^M \frac{1}{N} \sum_{i=1}^N \frac{1}{3} \sum_{\alpha} \langle \Phi_0^{(m)} | S_i^{\alpha} \frac{1}{\omega - H^{(m)}} S_i^{\alpha} | \Phi_0^{(m)} \rangle, \quad (2)$$

where M is the number of realizations of disorder, $|\Phi_0^{(m)}\rangle$ denotes the ground state for the J_{ij} set corresponding to the m -th realization, and $\alpha = x, y, z$ labels the three components of the spin operator. Although we deal with systems having a finite number of poles for each realization, the average over disorder naturally produces smooth response functions without need of introducing an artificial broadening as in usual exact diagonalization methods. In some cases, we found useful to use a logarithmic discretization of the ω -axis to obtain accurate results due to the large number of poles occurring at low frequencies.

To study the physical behavior at finite T , we exactly diagonalized the full hamiltonian matrix $H^{(m)}$. Each subspace belonging to the different S^z representations is separately diagonalized in order to optimize the use of memory. In this case, the local spin susceptibility is obtained from the spectral function

$$\begin{aligned} \chi''_{loc}(\omega) = & \frac{1}{M} \sum_{m=1}^M \frac{1}{N} \sum_{i=1}^N \frac{1}{Z^{(m)}} \sum_{k,l} |\langle \Phi_k^{(m)} | S_i^z | \Phi_l^{(m)} \rangle|^2 [\exp(-\beta E_k^{(m)}) \delta(\omega - (E_k^{(m)} - E_l^{(m)})) \\ & - \exp(-\beta E_l^{(m)}) \delta(\omega - (E_l^{(m)} - E_k^{(m)}))], \end{aligned} \quad (3)$$

where $\chi''_{loc}(\omega) = -2/\pi \text{Im}[\chi_{loc}(\omega)]$, while $E_k^{(m)}$ is the eigenenergy of the eigenstate $|\Phi_k^{(m)}\rangle$ corresponding to the m -th realization of disorder, $\beta = 1/T$ is the inverse of the temperature and $Z^{(m)}$ is the ensuing partition function.

The spin-glass phase is signaled by the divergence of the spin-glass susceptibility χ_{SG} , which is related to the local-spin susceptibility by [1]

$$\chi_{SG} = \frac{\chi_{loc}^2}{1 - J^2 \chi_{loc}^2}, \quad (4)$$

where $\chi_{loc} = \text{Re}[\chi_{loc}(\omega = 0)]$. Thus, the condition

$$J\chi_{loc} = 1 \quad (5)$$

indicates the instability of the system towards a spin glass state.

In previous papers [10,11] it was demonstrated the accuracy of the method by reproducing several known results for the infinite-range Ising model with random exchange interactions and transverse magnetic field Γ [19]. In particular, an accurate estimate for the critical value of the transverse field Γ_c , at which a quantum transition between the spin-glass and the paramagnetic phases takes place, was obtained. At finite T we should also test the accuracy of this approach for the current model we are studying. There are not many well known results that can be used for benchmark of this numerical method. To the best of our knowledge, the only quantitative prediction is $T_g \approx 0.14J$ for the critical temperature at which the spin-glass to paramagnetic phase transition occurs. This estimate was obtained by quantum Monte Carlo numerical solution [13] of the mean-field equations derived by Bray and Moore [12].

Results for the behavior of χ_{loc} as a function of T are shown in Fig. 1. The curve with circles correspond to extrapolations to the thermodynamic limit obtained from data for systems with up to $N = 12$ spins. At high temperatures, the local susceptibility obeys a Curie law, as expected. The asymptotic behavior $\chi_{loc} = \beta/4$ is plotted in dashed lines for comparison. As the temperature decreases, quantum fluctuations cause the reduction of the effective local magnetic moment and the response at $\omega = 0$ becomes smaller than that of classical spins. The condition (5) is satisfied at the critical temperature $T_g \approx 0.13$ where the systems begin to freeze. The diamond over the curve indicates the corresponding result obtained with quantum Monte Carlo [13] that shows very good agreement and validates our approach at finite T .

In Fig. 2 we show the behavior of χ_{loc} as a function of $1/N$ for a selected set of temperatures. A linear fit was performed to obtain the extrapolated values at $1/N = 0$. Error bars in Fig. 1 indicate the corresponding standard deviation. Interestingly, an even-odd effect is observed at temperatures below T_g , which suggests a change in the scaling law as the system enters the ordered phase.

III. THE DYNAMICAL SPIN RESPONSE.

A. $\chi''_{loc}(\omega)$ at $T = 0$.

Let us begin with the study of the spin response at $T = 0$. In this subsection we shall summarize and extend our recent results of Ref. [10].

The spectral function $\chi''_{loc}(\omega)$ is plotted in Fig. 3 for systems of different sizes. As we discussed in our previous paper [10], the most prominent feature is the existence of a $\sim \delta(\omega)$ piece plus a low frequency hump mounted on a regular contribution. Here, we shall present a more detailed analysis of the various contributions to $\chi''_{loc}(\omega)$, including some new excitations that were not previously noticed. We shall present just an heuristic, by no means rigorous, mathematical description of the different contributions to χ''_{loc} that will provide us with an appealing physical picture.

To gain insight on the nature of the dynamical response we analyzed individual realizations of disorder. We distinguished four different contributions which we shall describe in detail throughout this section:

$$\chi''_{loc}(\omega) = K\delta(\omega) + \chi''_{low}(\omega) + \chi''_{high}(\omega) + \chi''_{inc}(\omega), \quad (6)$$

where $\chi''_{low}(\omega)$ corresponds to the low frequency hump, $\chi''_{high}(\omega)$ indicates a feature at high frequency $\mathcal{O}(J)$ carrying a small spectral weight, while $\chi''_{inc}(\omega)$ denotes the contribution of excitations of incoherent nature which conform a quantum disordered paramagnetic background.

We will discuss the physical nature of all these contributions next. We begin with the latter that is due to incoherent excitations. We found that it can be described with the following simple expression

$$\chi''_{inc}(\omega) = C \exp\left[-\frac{\omega^2}{2J^2 S(S+1)}\right], \quad (7)$$

with $S = 1/2$ and C a constant. This function is plotted in thick line in Fig. 3 along with our results for $\chi''_{loc}(\omega)$.

We now show that this contribution can be heuristically described as independent spins in the presence of effective randomly fluctuating magnetic fields \mathbf{h} . We stress that we were not able to derive any proper demonstration of the validity of this procedure and we include it here with the sole hope of motivating the reader and perhaps providing new insights. The fields are the molecular fields at each site due to the action of all other spins,

$$\mathbf{h} = \frac{1}{\sqrt{N}} \sum_{i,j} J_{ij} \mathbf{S}_j. \quad (8)$$

Following standard arguments [1], we assume that for a given realization of disorder, they point to any spatial direction with equal normal probability

$$P(h) \propto \exp[-\frac{h^2}{2\sigma^2}], \quad (9)$$

where the variance σ can be taken to be $\sigma^2 = \langle \mathbf{h} \cdot \mathbf{h} \rangle \approx J^2 S(S+1)$.

We now recall that a spin under a magnetic field has a dynamical response given by

$$\chi''_o(\omega, h) = \frac{1}{3} [\frac{1}{4} \delta(\omega) + \frac{1}{2} \delta(\omega - h)], \quad (10)$$

where the finite frequency transverse part depends only on the magnitude of the field h .

Finally, we may combine (9) and (10) to obtain the incoherent background part of the dynamical spin response function within this heuristic picture

$$\chi''_{inc}(\omega) \propto \int_{-\infty}^{+\infty} dh P(h) \chi''_o(\omega, h), \quad (11)$$

that leads to (7) where the constant $C = 0.175$ is set to fit the numerical data. We carefully examined systems of several sizes and found that C varies negligible with N . A point we would like to make is that the averaging (11) involves a one-dimensional integral. The reason is that we are describing the quantum disordered regular contribution, therefore these fields cannot be assumed to have a fixed direction in space.

Another interesting observation is that this contribution to the response function, is very similar to one found in the spin-liquid phase of the $SU(M)$ generalization of the model at large M and in the quantum disordered regime (small S) [14–16].

In order to study the remaining three pieces of $\chi''_{loc}(\omega)$ in more detail, we subtract $\chi''_{inc}(\omega)$ from this quantity and define

$$\delta\chi''_{loc}(\omega) = \chi''_{loc}(\omega) - \chi''_{inc}(\omega). \quad (12)$$

This quantity exhibits a strong dependence on the system size N and a careful finite size analysis is necessary in order to extract reliable conclusions.

The $K\delta(\omega)$ part is a direct consequence of the $SU(2)$ rotational invariance of the Hamiltonian. To demonstrate this we sorted out the contributions to $\delta\chi''_{loc}(\omega)$ coming from the different S -sectors. In Fig. 4 we show results for the $S = 0$, $S = 1$ and $S = 2$ sectors. A remarkable observation is that the $\sim \delta(\omega)$ part is absent in the $S = 0$ case, while present in the remaining $S \neq 0$ sectors. Moreover, the systematic analysis of histograms of S (cf. Fig. 5a) for increasing N , reveals that $\langle S \rangle \propto \sqrt{N}$ as shown in Fig. 5b. Therefore, although the mean total spin $\langle S \rangle \neq 0$ in the thermodynamic limit (in fact diverges), the local magnetization, i.e. the magnetization *per site* $\langle S \rangle / N \rightarrow 0$. We have thus traced the origin of this $\sim \delta(\omega)$ feature to a “soft mode” connecting the $2S+1$ -fold degenerate ground state that persists in the $N \rightarrow \infty$ limit.

The low frequency hump $\chi''_{low}(\omega)$ evolves towards a narrowing feature at $\omega = 0$ that becomes a δ -function in the thermodynamic limit. In fact, the spectral weight of this part contributes together with K to the Edwards-Anderson order parameter q . To elucidate the origin of this hump, we looked carefully to the structure of the ground state wave function for realizations of disorder that yielded spectral weight in the energy range of the hump $\chi''_{low}(\omega)$. We found that in those realizations the ground state wave function is dominated by some large amplitudes of just a few pairs of states. The states conforming a pair are related by a time-reversal operation [20]. They appear in a symmetric (when $N/2$ is even) or antisymmetric (when $N/2$ is odd) linear combination. Moreover, we also observed that most of the individual spin states in each of the two states of a given pair are in a configuration compatible with the particular realization of J_{ij} interactions. Thus we can think of this large fraction of spins as defining an unfrustrated cluster of

size N_c ($\mathcal{O}(N)$). Therefore, several unfrustrated clusters are defined for each realization of disorder. In fact, a number equal to the number of dominating pair of amplitudes occurring in the ground state wave function. An appealing picture to visualize the ground state is that the clusters undergo a quantum mechanical tunneling back and forth between the two corresponding pair of states. As many pairs coexist in any given ground state, then the picture is that many unfrustrated cluster simultaneously undergo these quantum oscillations.

With this physical picture of the ground state in mind it should not be hard to anticipate that the excitations that contribute to $\chi''_{low}(\omega)$ (the hump) are nothing but wave functions where one (any) of the clusters has its pair of associated amplitudes appearing with the opposite symmetry respect to that in the ground state (a “flipped” cluster). Since many coexistent clusters occur in a single ground state for a given realization, then there are many corresponding excited states contributing to the hump. We can think of these as real collective excitations, as they involve the simultaneous change in the state of a large number of individual spins. We have confirmed this qualitative picture by direct inspection of the amplitudes of the wave functions of the excited states in many realizations of disorder.

An important observation that we made is that the difference in energy between the ground state and the excitations is small (we found it to be $\mathcal{O}(1/N)$). Thus, these collective excitations become degenerate with the ground state and contribute with a sizable weight to the dynamical spin response at $\omega = 0$ in the thermodynamic limit. In other words, the hump collapses into a δ -function contribution in that limit. A side consequence of this observation is that even within the $S=0$ sector, which also shows a hump in the dynamical response, the $T=0$ state is that of a spin-glass with local magnetizations with long range order in time.

To perform a quantitative analysis of the behavior of $\chi''_{low}(\omega)$ as a function of N , we used the following parametrized form

$$\chi''_{low}(\omega) = A \exp[-\frac{\omega^2}{\Gamma^2}]. \quad (13)$$

and tracked the systematic evolution of the parameters as function of temperature and system size.

Typical curves are shown in Fig. 6 for two different sizes. The fitting parameters A and Γ have a strong dependence on the system size. Their behavior as functions of $1/N$ is shown in Fig. 7. The width Γ obeys a linear extrapolation to 0, while the integral of $\chi''_{low}(\omega)$ (squares in Fig. 7) remains approximately constant. This provides further quantitative support to the claim that $\chi''_{low}(\omega)$ evolves to a $\sim \delta(\omega)$ contribution in the thermodynamic limit. The integrated spectral weight provides an estimate for the Edwards-Anderson order parameter q . With this procedure it is found $q \sim 0.04$, which improves upon our previous estimate $q \sim 0.06$ [10]. We shall later discuss the origin of this difference.

To complete this subsection, we turn to discuss a last and small contribution to $\chi''_{loc}(\omega)$, the high frequency part $\chi''_{high}(\omega)$. This piece of the spectral function is related with the existence of a spin-glass order and it is essentially the high energy counterpart of $\chi''_{low}(\omega)$. Similar to the former case, $\chi''_{high}(\omega)$ is due to excitations of the clusters. But the key difference is that now the excitations are incoherent in nature, involving the unbinding of single spins out of the unfrustrated clusters. The spins will then independently revolve around its local field with a fast precession frequency. In other words, the relevant excitations contributing to $\chi''_{high}(\omega)$ correspond to the flipping of individual spins out of the large unfrustrated clusters.

An heuristic mean field picture can also be presented in this case. To describe these processes let us think of an originally unfrustrated cluster of N_c spins as being made of a single spin plus the remaining cluster of $N_c - 1$ correlated spins. The latter would produce an effective magnetic field pointing to some fixed (or very slowly moving) direction which couples to the single spin that will undergo a fast precession around the slow effective field due to the cluster. To estimate the magnitude of the effective field $h = |\mathbf{h}|$, we assume it to be normally distributed around $h_0 = |\sum_{ij} J_{ij} \mathbf{S}_j|/\sqrt{N}$, which is a quantity of $\mathcal{O}(J)$. Therefore, similarly as we did before for $\chi''_{inc}(\omega)$, we can perform the average over the disorder as an average over the distribution of effective fields, to obtain the contribution of $\chi''_{high}(\omega)$ from

$$\chi''_{high}(\omega) \propto \int_0^{+\infty} dh h^2 P(h) \chi''_o(\omega, h), \quad (14)$$

with $\chi''_o(\omega, h)$ of the form (10) where we point out that in the present case, the directions of the effective fields are now *frozen* and thus we include the h^2 term of the Jacobian of $d\mathbf{h}$.

The integral leads to the following functional form for this high frequency incoherent contribution,

$$\chi''_{high}(\omega) = B \omega^2 \exp[-\frac{(\omega - h_0)^2}{2\sigma^2}]. \quad (15)$$

We were not able to determine h_0 and the variance σ of the probability distribution analytically. These parameters and the constant B can be chosen to fit the numerical data, however, the sizable finite size effects observed and the

small spectral intensity did not allow us for a very accurate determination. We found that the choice of $h_0 = 1$ and $\sigma = 0.5$ is consistent with the behavior of $\chi''_{high}(\omega)$ as the system grows to the large size limit, as shown in Fig. 8. We note that the spectral weight of this contribution is extremely small, less than 5 percent of the total weight of $\chi''(\omega)$, which implies that the agreement remains only qualitative.

A final issue that we would like to discuss briefly concerns the difference in the estimated value for the Edwards Anderson order parameter q , in comparison with the result we reported in Ref. [10]. This has a simple explanation: the $T = 0$ sum rule $\int d\omega \chi''(\omega) = 1/4$ is used to numerically compute the order parameter from the expression

$$q = \frac{1}{4} - \int_0^\infty d\omega \chi''_{reg}(\omega), \quad (16)$$

where $\chi''_{reg}(\omega)$ denotes the regular part of the spectral function. We have already discussed the many different contributions to the $\chi''_{reg}(\omega)$, including the small last one from $\chi''_{high}(\omega)$, which went unnoticed in our previous work [10]. The spectral weight carried by $\chi''_{high}(\omega)$ is only ~ 0.015 and is in fact the origin and amount of the difference. We have now achieved a better and more accurate description of the regular part of the frequency dependent spin-spin response function that through (16) enabled us to obtain a more accurate estimate for the order parameter q .

B. $\chi''_{loc}(\omega)$ at finite T .

We now turn to the behavior of the dynamic response at finite temperature. We recall the definition of the spectral density $\rho(\omega)$,

$$\rho(\omega) = \frac{1}{e^{-\beta\omega} - 1} \chi''_{loc}(\omega). \quad (17)$$

It is more convenient to use $\rho(\omega)$ instead of $\chi''_{loc}(\omega)$. While both quantities coincide at $T = 0$, the former obeys a simple sum-rule which allows for a clearer interpretation of the transfer of spectral weight. In fact, the sum-rule reads

$$\int_0^\infty \rho(\omega) d\omega = \frac{1}{4}. \quad (18)$$

The heuristic derivation of a response function for the incoherent degrees of freedom that we presented before can be easily extended to finite temperatures. We obtain

$$\chi''_{inc}(\omega, T) = C \exp\left[-\frac{\omega^2}{2JS(S+1)}\right] \tanh\left(\frac{\beta\omega}{2}\right). \quad (19)$$

and correspondingly,

$$\rho_{inc}(\omega, T) = C \exp\left[-\frac{\omega^2}{2JS(S+1)}\right] \tanh\left(\frac{\beta\omega}{2}\right) \frac{1}{e^{-\beta\omega} - 1}. \quad (20)$$

where the constant C is now $C = C(T)$. Rather remarkably, the analysis of our results demonstrate that the functional form for $\rho_{inc}(\omega, T)$ remains an excellent fit for the incoherent part of the spectra. Moreover, we found that within the temperature range investigated (0 to $\sim 2T_g$) the numerical value of the coefficient C remains a constant within our numerical precision. We should mention, however, that at high enough temperature, at least the numerical value of C has to change for the fit to comply with the sum-rule. The rather uninteresting high temperature regime has been left out from the scope of the present work.

Similarly as we did before, we use the expressions above to guide our analysis of the numerical data. We define

$$\delta\rho(\omega, T) = \rho(\omega, T) - \rho_{inc}(\omega, T). \quad (21)$$

Typical curves for $T = 0.25$ are depicted in Fig. 9 for different system sizes. As in the case of $T = 0$ the response is split in a low frequency feature and a higher frequency one. The low frequency peak corresponds to the δ -function contribution discussed at $T = 0$ that now acquires a *finite* width ($\mathcal{O}(T)$) due to the slow diffusive modes that appear at finite temperatures.

A last and smaller contribution is also apparent at higher frequencies of $\mathcal{O}(J)$. It is nothing but the signature of the high frequency contribution that we discussed at the end of the previous subsection. It corresponds to the

fast precession of single unbinded spins around the now slowly varying magnetic fields. While the physical picture is qualitatively clear, we were not able to perform reliable extrapolations to the thermodynamic limit to extract quantitative detailed results upon the evolution of the spectrum as T increases. In particular, it was not possible to obtain an accurate estimate of the Edwards-Anderson order parameter as a function of T . While no technical impediment exists a priori with the method, it turns out that the statistics that we collected were not sufficient. These details will have to wait for longer runs or more powerful computational resources. A final point we would like to consider is the transfer of spectral weight. Although the size of our systems is limited to 12 sites, this seems to be sufficient for a qualitative discussion the evolution and transfers of spectral weight of $\rho(\omega)$ as a function of temperature.

In Fig. 10 we show results for $\delta\rho(\omega, T)$ at temperatures in the range of 0.04 to 0.25. One may think of this contribution to the spectra as due to the slow degrees of freedom that were originally frozen at $T = 0$ and then gradually melt as T is increased. Our results indicate that the width of the low frequency peak is linear in T , as may be expected for diffusive modes [21]. Interestingly, the small higher frequency part is a rather broad feature that does not show any significant shift nor broadening with temperature, but merely loses spectral intensity with increasing T . At finite T , the effect of the gradual melting of the clusters of frozen spins leads to a slow (diffusive) motion of the directions in which they point. However, as long as the drift of those clusters is slow compared to the fast precession of the unbinded spins, the higher frequency contribution should remain approximately unchanged, except for its spectral intensity which decreases with T .

This brings us to a last issue worth mentioning, namely, the transfer of spectral weight towards the background when $T > T_g$. This feature is better seen in the integrals

$$I(\omega, T) = \int_{-\infty}^{\omega} d\omega' \rho(\omega', T), \quad (22)$$

which are shown in Fig. 11 for the same set of temperatures as in Fig. 10.

It is clear in Fig. 11 that as the temperature increases, the distinction between low and high degrees of freedom gradually disappears and that the width of the main feature grows towards the single bare energy scale of the model J that must control the physics at high temperatures.

IV. THE SPECIFIC HEAT.

In real materials with a spin-glass phase below T_g , the specific heat C_v exhibits a smooth maximum well above the critical temperature [1,7,8]. The origin of this behavior remains an open question as it cannot be explained from the predictions of classical models. In particular, for the Sherrington Kirpatrick model [22], which is the classical version of the Heisenberg model, it is found that C_v has a maximum exactly at T_g^{SK} with a small discontinuity in $\partial C_v / \partial T$ [8]. In this section we shall argue that the observed behavior of C_v can be understood as a result of quantum effects. We shall discuss the role of quantum fluctuations in the behavior of the specific heat

$$C_v = \frac{\partial E}{\partial T}. \quad (23)$$

and show that it leads to a shift of the maximum of C_v towards temperatures higher than T_g .

The mean value of the energy per spin E is computed from

$$\begin{aligned} E &= \frac{1}{N} \frac{1}{M} \sum_{m=1}^M \frac{1}{Z^{(m)}} \sum_k [e^{-\beta E_k^{(m)}} E_k^{(m)}] \\ &= \int_{-\infty}^{+\infty} d\omega \omega \chi''_{loc}(\omega), \end{aligned} \quad (24)$$

and (23) is obtained by numerically differentiating this quantity. The energy E as a function of T is shown in Fig. 12 for several system sizes. In the spirit of the previous analysis of the different contributions to $\chi''_{loc}(\omega)$ and using expression (24), we may think of E as resulting from two different contributions: $E = E_{inc} + E_{coh}$. The energy E_{inc} comes from the fraction of degrees of freedom that remain unfrozen down to $T = 0$ due to quantum fluctuations, and E_{coh} is the gain in energy due to the formation of the glass. As it turns out, the former is the largest contribution of the two and is obtained by replacing (19) in (24)

$$E_{inc} = C \int_{-\infty}^{+\infty} dh h \exp\left[\frac{-h^2}{2J^2 S(S+1)}\right] \tanh\left(\frac{\beta h}{2}\right). \quad (25)$$

This energy is indicated in thick line in Fig. 12. At low temperatures it underestimates (in absolute value) the total E as it lacks the sizeable contribution from the frozen degrees of freedom. On the other hand, at higher temperatures its qualitative behavior is similar to that of $E(T)$.

The results for $C_v(T) = \partial E / \partial T$ are shown in Fig. 13 for systems of various sizes. The contribution of the incoherent background is also plotted in thick line for comparison. It is remarkable that C_v exhibits a smooth cusp with a maximum at a temperature $T_M \approx 0.25$ which is significantly larger than T_g . Interestingly, the contribution of the incoherent background exhibits a similar maximum at approximately T_M . The actual contribution to C_v coming from the frozen part is relatively small compared to the quantum disordered part. Thus, the latter is found to dominate the behavior of C_v and in fact it predominantly determines the actual position of the maximum.

Therefore, our results strongly suggest that in the present model incoherent mean-field like excitations due to quantum fluctuations set the behavior of C_v as a function of T . In real systems the quantum fluctuations (controlled by, for instance, anisotropy) may play a more or less important role than in the current model but should always be present. One may thus expect that its effect could produce larger or smaller shifts of T_M always to higher temperatures respect to T_g , as is in fact observed experimentally.

To give further support to our claims, we investigate the finite size effects on C_v in more detail. We applied the same numerical procedure to the classical Sherrington-Kirpatrick model [22], which is defined by the hamiltonian

$$H_{SK} = \frac{1}{\sqrt{N}} \sum_{i,j=1}^N J_{ij} S_i^z S_j^z. \quad (26)$$

where S_i^z denote Ising spins now. This model has been extensively studied and many well established results have been reported in the paramagnetic and glassy phases [1,7,8]. Results for the behavior of C_v as a function of T obtained with exact diagonalization are shown in Fig. 14 for systems of various sizes. Although these data does not allow us to capture a subtle issue such as the small cusp in C_v at T_g^{SK} in the thermodynamic limit, it is clear that the curves become sharper as the size of the system increases. More remarkable is the fact that for these finite systems the maximum T_M occurs *below* T_g , in marked contrast with the behavior of C_v in the random Heisenberg model that is also depicted in the figure for comparison. Note that the finite size effects on T_M in the quantum model are negligible.

We therefore conclude that our results show strong evidence that the smooth maximum of C_v at $T_M > T_g$ is a genuine feature of the quantum model rather than a finite size effect.

V. SUMMARY AND DISCUSSION

In summary, we have studied the random infinite-range Heisenberg model at $T = 0$ and at finite temperature with exact diagonalization techniques by carrying out a careful analysis of the finite size effects. We have first shown that our approach is able to reproduce the sole well established quantitative result known to us in this model, namely, the quantum Monte Carlo estimate of the critical temperature T_g [13] for spin glass ordering.

At $T = 0$ we found that the dynamical spin response in the thermodynamic limit behaves as $\chi''_{loc}(\omega) = q\delta(\omega) + \chi''_{reg}(\omega)$, where q is the Edwards Anderson parameter. The low energy excitations producing the $\propto \delta(\omega)$ response are due to two different contributions. On one hand, the freezing of slow collective excitations that we identified as groups of spins that build unfrustrated clusters and coexist in a given typical realization of disorder. The nature of these excitations is the slow quantum tunneling between (cluster) states related by a time-reversal operation. On the other hand, there is also a second contribution to the $\propto \delta(\omega)$ response due to a 0-mode like excitation originated in the spin-rotation invariance of the model and the fact that there is a finite mean total spin. Interestingly, while the local magnetic moment of the system, i.e. the mean magnetic moment *per site*, does vanish in the thermodynamic limit, we found that the total spin is $S \neq 0$ and of $\mathcal{O}(\sqrt{N})$.

The regular part $\chi''_{reg}(\omega)$ collects the contribution of incoherent excitations due to quantum fluctuations plus the effect of high energy excitations due to the flipping of some few unbinded spins. Both kinds of excitations seem to be very well described in terms of heuristic mean-field theories that provide a qualitative insight.

When the temperature T increases the response of the low energy excitations is found to acquire a finite width of order T due to the melting of frozen spins. As these degrees of freedom gradually unbind and become part of the regular contribution, the weight of the high energy excitations gets also gradually reduced. However, the shape of this part of the response is preserved within a wide temperature range as long as there is a separation of energy scales between the slow and fast excitations.

We have also studied the behavior of the specific heat as a function of T . We found compelling evidence that in the thermodynamic limit C_v has a smooth maximum at a temperature T_M , significantly larger than the transition temperature T_g . This behavior is in excellent qualitative agreement with that experimentally observed in real spin

glasses and is in marked contrast with the predictions based on classical models such as the Sherrington-Kirpatrick hamiltonian. We have shown that the origin of the unusual behavior can be traced to the excitations due to quantum disorder which dominate the behavior of the specific heat.

In conclusion, based in our numerical analysis, the picture we propose for the spin-glass state is that a fraction of the system forms coexisting unfrustrated clusters which are frozen or undergoing a slow collective motion. The rest of the system remains in an uncorrelated incoherent state mostly described by local spin dynamics. Such a picture manifests itself in the different contributions to the dynamical response and particularly in $C_v(T)$, since the incoherent excitations produce a smooth variation in the specific heat and this quantity does not show any signature of the paramagnetic to spin-glass transition. We find that this picture can be quite general and that it provides a possible explanation for the behavior of the specific heat in real materials which remained, so far, a standing question in the physics of spin glass systems.

Another interesting observation is that the solutions of the $SU(M)$ generalization of the model treated in the large M limit produces several qualitatively different phases depending on the value of the "size" of the spin, S [14–16]. In particular, for large S the system is in a spin-glass state with a dynamic response that has a δ -function at $\omega = 0$, while for $S \rightarrow 0$ the system goes into a spin-liquid state with a response function that remains regular and goes to a constant at $\omega \rightarrow 0$. Therefore, under the light of our results, the large M limit of the model seems to capture, in its different regimes, several aspects present in the $M=2$ solution.

From the technical point of view, we can say that the present approach offers a very appealing alternative for the study of disordered systems. Without the need of approximations, it enables the treatment of paramagnetic and disordered phases on equal footing and provides a deep insight on the nature of the relevant excitations. At least for the present model, we were able to find reliable extrapolations to the thermodynamic limit for most of the studied quantities, thus overcoming the obstacle of the finite-size effects of the systems under study.

Finally, many interesting issues are left for future work, such as a systematic study of the role of dimensionality or lattice connectivity and that of anisotropy.

VI. ACKNOWLEDGEMENTS

L. A. thanks G. Santoro for his comments on this manuscript. We acknowledge support from CONICET and from grants of ANCyPT, Fundación Antorchas and ECOS-SECyT.

-
- [1] K.H.Fischer and J.A.Hertz, *Spin Glasses*, Cambridge University Press, Cambridge, England (1991).
 - [2] S. Sachdev, *Quantum Phase Transitions*, Cambridge University Press, Cambridge, England (1999).
 - [3] D.H.Reich *et al.*, *Phys. Rev. B* **42**, 4631 (1990). W. Wu *et al.*, *Phys. Rev. Lett.* **67**, 2076 (1991). W. Wu *et al.*, *Phys. Rev. Lett.* **71**, 1919 (1993).
 - [4] J.Brooke, D.Bitko, T.F.Rosenbaum and G.Aeppli, *Science* **284**, 779 (1999).
 - [5] Urano *et al.*, *Phys. Rev. Lett.* **85** 1052 (2000).
 - [6] E.Dagotto, *Rev.Mod.Phys.* **66**, 763 (1994).
 - [7] H.Rieger und A.P.Young, *Quantum Spin Glasses*, Lecture Notes in Physics **492** "Complex Behavior of Glassy Systems", p. 254, ed. J.M. Rubi and C. Perez-Vicente (Springer Verlag, Berlin-Heidelberg-New York, 1997).
 - [8] K.Binder and A.P.Young, *Rev.Mod.Phys.* **58**, 801 (1986).
 - [9] G.Parisi, *Phys. Rev. Lett.* **23**, 1754 (1979).
 - [10] L.Arrachea and M.J.Rozenberg, *Phys. Rev. Lett.* **86**, 5172 (2001).
 - [11] M. J. Rozenberg and L. Arrachea, *Physica B* (in press).
 - [12] A.J.Bray and M.A.Moore, *J. Phys. C* **13**, L655 (1980).
 - [13] D.R.Grempel and M.J.Rozenberg, *Phys. Rev. Lett.* **80**, 389 (1998).
 - [14] S. Sachdev and J. Ye, *Phys. Rev. Lett.* **70**, 3339 (1993).
 - [15] A. Georges, O.Parcollet and S. Sachdev, *Phys. Rev. Lett.* **85**, 840 (2000).
 - [16] A. Georges, O.Parcollet and S. Sachdev, *Phys. Rev. B* **63**, 134406 (2001).
 - [17] E.R.Gagliano, E.Dagotto, A.Moreo and F.C.Alcaraz, *Phys. Rev. B* **34**, 1677 (1986).
 - [18] L. Arrachea, *Phys. Rev. B* **62** 10 033 (2000).
 - [19] M.J.Rozenberg and D.R.Grempel, *Phys. Rev. Lett.* **81**, 2550 (1998).
 - [20] We focus our discussion to ground states with $S = 0$, adopting a basis within the $S^z = 0$ representation. Nevertheless, our arguments can be generalized to the other spin components.

- [21] D. Forster. Hydrodynamic Fluctuations, Broken Symmetry, and Correlation Functions, Ed. Addison Wesley, (1994).
- [22] D.Sherrington and S.Kirkpatrick, Phys. Rev. Lett. **35**, 1972 (1975).

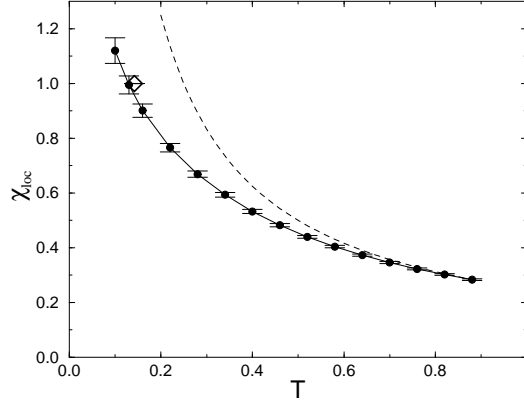


FIG. 1. The $\omega = 0$ dynamical susceptibility χ_{loc} as a function of T . Solid circles correspond to extrapolations of the numerical data to the thermodynamic limit (error bars are indicated). The critical temperature T_g corresponds to $\chi_{loc} = 1$. The diamond corresponds to the result of the Monte Carlo solution of Bray and Moore equations. The Curie law followed by classical spins is shown in dashed lines.

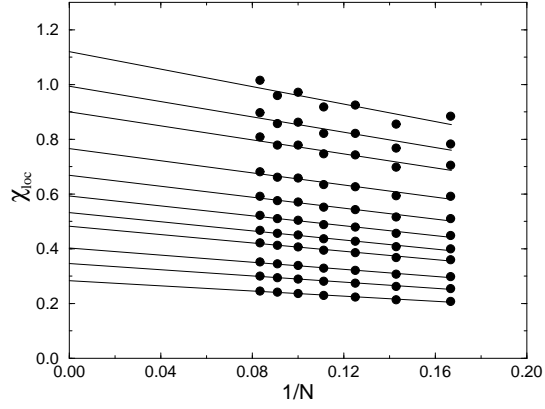


FIG. 2. χ_{loc} as a function of $1/N$ for different temperatures above and below T_g . The corresponding temperatures are $T = 0.1, 0.13, 0.16, 0.22, 0.28, 0.34, 0.4, 0.46, 0.58, 0.7, 0.88$ (top to bottom). Solid lines show the linear fitting to perform the extrapolation to the thermodynamic limit.

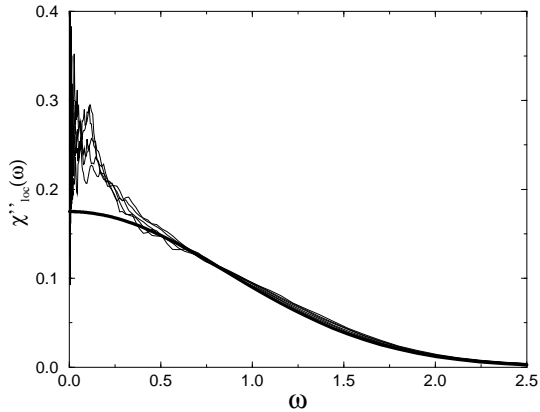


FIG. 3. The spectral function $\chi''_{loc}(\omega)$ for systems of 8, 10, 12, 14 and 16 spins (bottom to top). The thick line indicates the response due to incoherent excitations given in Eq. (7), with $S = 1/2$. The constant $C = 0.175$ is set to fit the numerical data.

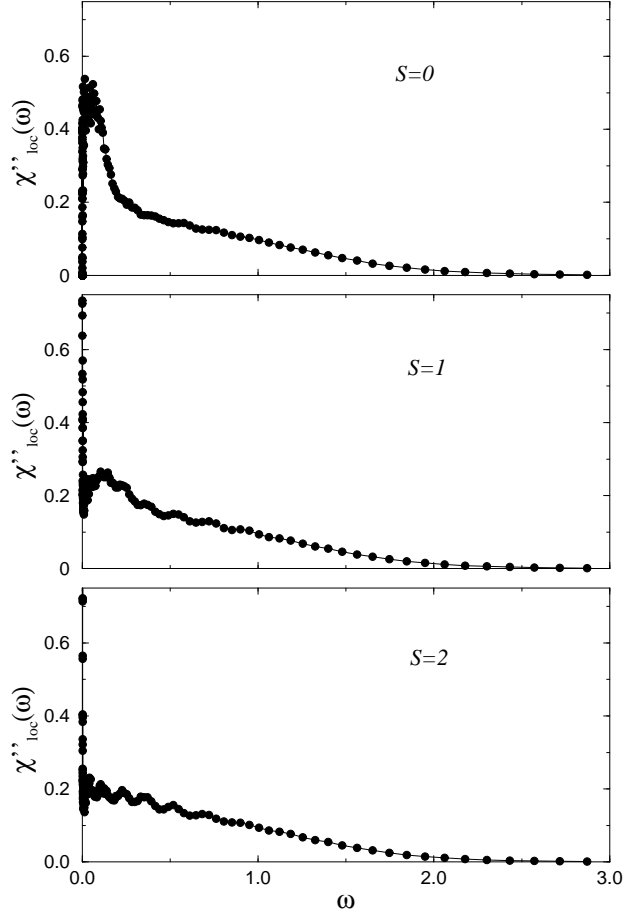


FIG. 4. The spectral function $\chi''_{loc}(\omega)$ for $N = 14$ corresponding to the average over the set of disorder realizations with the ground state in the $S = 0, 1, 2$ total spin sectors (top to bottom).

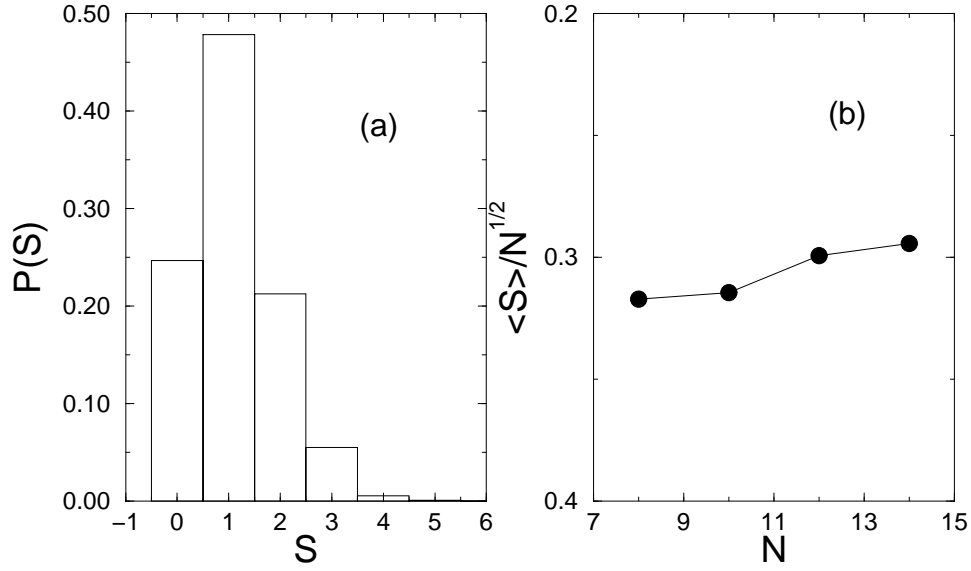


FIG. 5. (a) Histogram for the total spin S of the ground state for $N = 14$. (b) $\langle S \rangle / \sqrt{N}$ as a function of the system size.

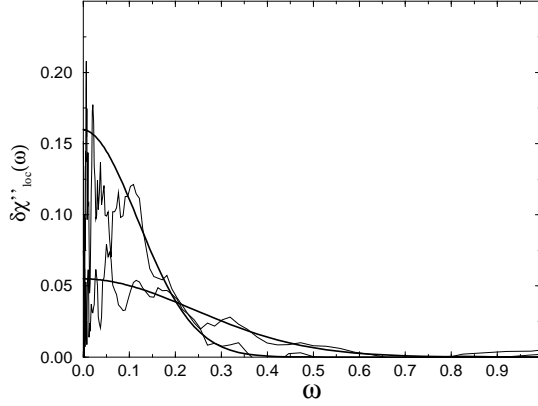


FIG. 6. Details of the low frequency part of $\delta\chi''_{loc}(\omega)$ for systems with $N = 6, 14$. The thick lines indicate the Gaussian fits to the numerical data.

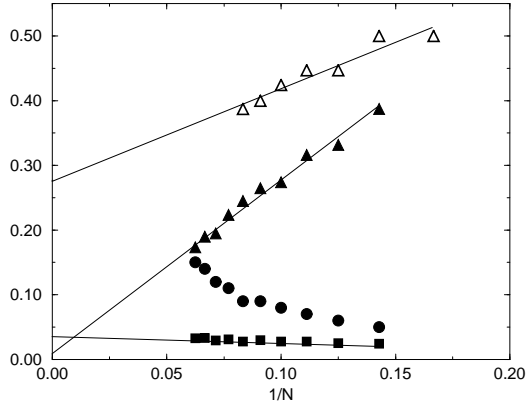


FIG. 7. The parameters of the Gaussian fitting function for the low frequency contribution to the response as a function of the inverse system size $1/N$. The circles correspond to the height A and the triangles to the width Γ of the Gaussian defined in Eq. (13). The squares indicate the spectral weight of χ''_{low} .

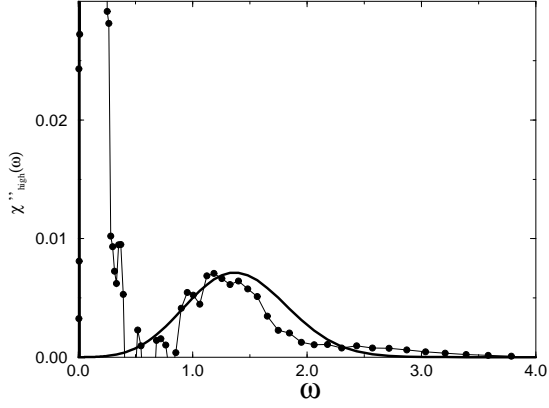


FIG. 8. Details of the high frequency part of $\delta\chi''_{loc}(\omega)$ for a system of 14 spins. The thick line corresponds to $\chi''_{high}(\omega)$ given by Eq.(15) with $B = 0.005$, $\sigma = 1/2$ and $h_0 = 1$. The spectral weight of this contribution is small, less than 5% of the total spectral weight.

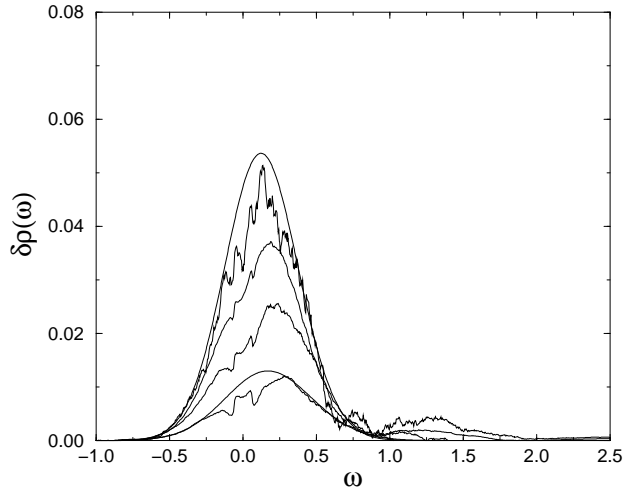


FIG. 9. $\delta\rho(\omega, T)$ for systems with $N = 6, 8, 10, 12$ sites at $T = 0.25$. Thick lines are fits with Gaussians times the function $1/(1 - \exp(-\beta\omega))$.

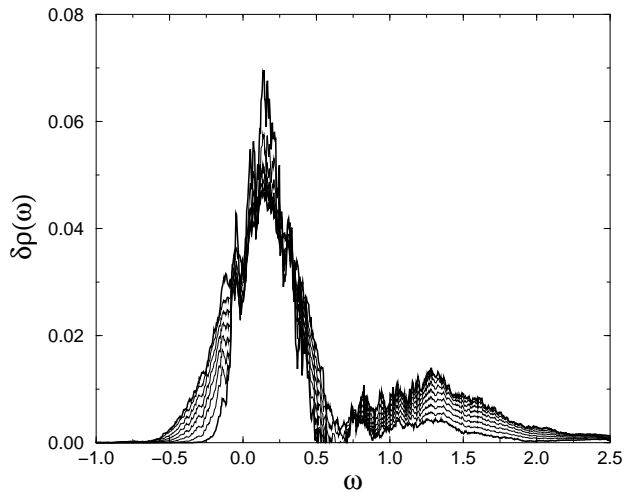


FIG. 10. $\delta\rho(\omega, T)$ for $N = 12$ and $T = 0.04, 0.7, 0.1, 0.13, 0.16, 0.19, 0.22, 0.25$ (bottom to top of lower frequency feature and top to bottom of the higher frequency one). The curves corresponding to the lowest and highest temperatures are indicated in thick lines.

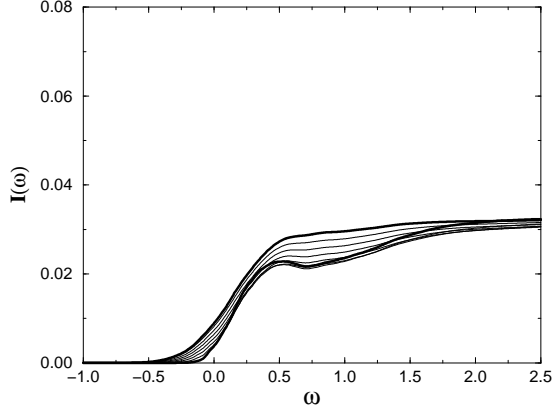


FIG. 11. The integrated spectral weight $I(\omega)$ defined in (22) for $N = 12$ and $T = 0.04, 0.7, 0.1, 0.13, 0.16, 0.19, 0.22, 0.25$ (bottom to top). The curves corresponding to the lowest and highest temperatures are indicated in thick lines.

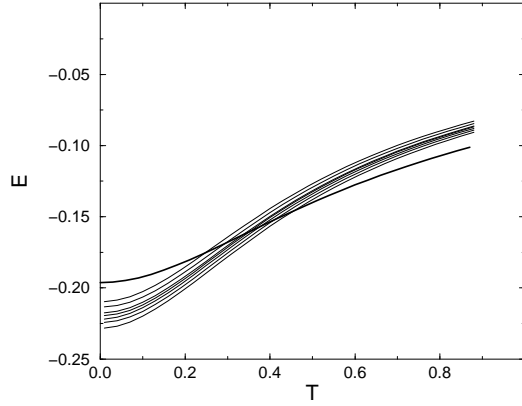


FIG. 12. The mean energy E defined in (24) as a function of T for systems with $N = 6, 7, 8, 9, 10, 11, 12$ (top to bottom) sites. The thick line corresponds to the contribution of the incoherent part (25).

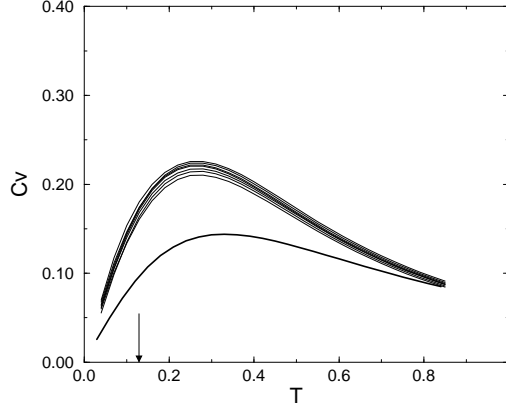


FIG. 13. The specific heat C_v defined in (23) as a function of T for systems with $N = 6, 7, 8, 9, 10, 11, 12$ (bottom to top) sites. The thick line corresponds to the contribution of the incoherent part. The arrow indicates the critical temperature T_g .

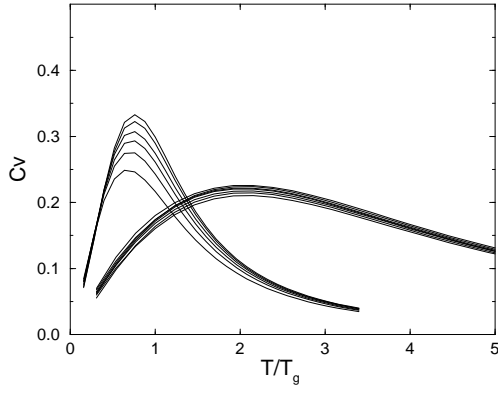


FIG. 14. The specific heat C_v as a function of T/T_g for systems with $N = 6, 7, 8, 9, 10, 11, 12$ (bottom to top) sites. The set of curves on the right corresponds to the Heisenberg model while the one on the left to the Sherrington Kirpatrick model (26).

